

Enhanced Electrochemical Property of Surface Modified $\text{Li}[\text{Co}_{1/3}\text{Ni}_{1/3}\text{Mn}_{1/3}]\text{O}_2$ by ZrF_x Coating

Su Hyun Yun and Yong Joon Park*

Department of Advanced Materials Engineering, Kyonggi University, Suwon 443-760, Korea

*E-mail: yjpark2006@kyonggi.ac.kr

Received November 25, 2009, Accepted December 18, 2009

A $\text{Li}[\text{Ni}_{1/3}\text{Co}_{1/3}\text{Mn}_{1/3}]\text{O}_2$ cathode was modified by applying a ZrF_x coating. The surface-modified cathodes were characterized by XRD, SEM, EDS, TEM techniques. XRD patterns of ZrF_x -coated $\text{Li}[\text{Ni}_{1/3}\text{Co}_{1/3}\text{Mn}_{1/3}]\text{O}_2$ revealed that the coating did not affect the crystal structure of the parent powder. SEM and TEM images showed that ZrF_x nano-particles were formed as a coating layer, and EDS data confirmed that ZrF_x distributed uniformly on the surface the powder. Capacity retention of coated samples at high C rates was superior to that of pristine sample. However, as the coating concentration increases beyond the optimum concentration, the rate capability was deteriorated. Whereas, as the increase of coating concentration to 2.0 wt %, the cyclic performances of the electrodes under the severe conditions (high cut-off voltage, 4.8 V, and high measurement temperature, 55 °C) were improved considerably.

Key Words: Cathode, ZrF_x , Surface coating, Lithium battery

Introduction

$\text{Li}[\text{Ni}_{1/3}\text{Co}_{1/3}\text{Mn}_{1/3}]\text{O}_2$ has been extensively investigated for its potential to replace LiCoO_2 currently used in Li secondary batteries, owing to its high discharge capacity and enhanced cyclic performances.¹⁻³ However, problems such as inferior rate capability and thermal stability must be overcome before $\text{Li}[\text{Ni}_{1/3}\text{Co}_{1/3}\text{Mn}_{1/3}]\text{O}_2$ can be used practically. In an attempt to overcome these problems, coating of the surface of the pristine powder of this compound with stable materials has been tried. According to some previous studies,⁴⁻¹⁰ coated cathode materials have shown enhanced electrochemical properties and thermal stability. Cho *et al.* reported that the coating resulted in reduced transition-metal dissolution during cycling,⁵ thus improving the discharge capacity and stable cyclic properties. Thackeray *et al.* suggested that the oxide coating can act as a highly Li-conductive solid-electrolyte interface and serve to scavenge and neutralize any HF species present in the electrolyte.⁶ Myung *et al.* also proposed that possible reason of improved battery performances by the metal oxide coating.^{4,7} They reported that the metal oxide coating layer transformed into a metal-fluoride layer during cycling, leading to greater resistance to HF attack during cycling. Although the reason for the improvement has not been completely understood yet, it is obvious that the coating method is very effective in countering several problems originating from the direct contact between the cathode and the electrolyte. However, the effectiveness of coating of cathode electrodes is highly dependent on the coating materials used.⁷⁻¹⁰ Therefore, identification of a suitable coating material is a key factor for obtaining highly improved cathode material by the process of coating. In this study, zirconium fluoride (ZrF_x) was used as a coating material for a $\text{Li}[\text{Ni}_{1/3}\text{Co}_{1/3}\text{Mn}_{1/3}]\text{O}_2$ cathode. Some fluoride-coated cathode was investigated for its enhanced electrochemical properties and thermal stability.¹¹⁻¹³ Moreover, Zr compound such as zirconium oxide has been investigated and found to be an excellent coating substituent.^{14,15} In the present study,

the ZrF_x surface modified $\text{Li}[\text{Ni}_{1/3}\text{Co}_{1/3}\text{Mn}_{1/3}]\text{O}_2$ cathodes were prepared and their electrochemical and structural properties were characterized.

Experimental

Pristine $\text{Li}[\text{Ni}_{1/3}\text{Co}_{1/3}\text{Mn}_{1/3}]\text{O}_2$ powder was supplied by ECO-PRO. For preparing the coating solution, $\text{Zr}(\text{CH}_3\text{CO}_2)_2 \cdot (\text{OH})_2$ (99.99%, Aldrich) and NH_4F (98%+, Aldrich) were firstly dissolved in distilled water, and then, the solution was stirred continuously for 2 h at 25 °C. The molar ratio of the Zr source to the F source was adjusted to 1 : 4 (ZrF_4). The surface coating was carried out by a typical wet process. $\text{Li}[\text{Ni}_{1/3}\text{Co}_{1/3}\text{Mn}_{1/3}]\text{O}_2$ powder was added to the coating solution and stirred at 80 °C for 2 h and dried in an oven at 100 °C for 12 h. Samples were then heat treated in a furnace at 400 °C for 5 h.

X-ray diffraction (XRD) patterns of powders were obtained using a Rigaku X-ray diffractometer in the 2θ range of 10 - 70° with monochromatized $\text{Cu-K}\alpha$ radiation ($\lambda = 1.5406 \text{ \AA}$). The microstructure of the powder was observed by field-emission scanning electron microscopy (FE-SEM, JEOL-JSM 6500F). Transmission electron microscopy (FE-TEM, JEOL-JEM 2100F) was also carried out using an electron microscope, operating at 200 kV. The cathodes to be used electrochemical studies were prepared using a doctor-blade coating method with a slurry of 80 wt % coated active material, 12 wt % conductive carbon (Super-P) and 8 wt % poly vinylidene fluoride (PVDF) with *N*-methyl-2-pyrrolidone (NMP), as the solvent for the mixture. The slurry was then applied to an aluminum foil current collector and dried at 90 °C in an oven. The coated cathode foil was cut into circular discs 12 mm in diameter. The electrochemical performances of the discs were evaluated with coin-type cells of the 2032 configuration and the discs were assembled in an argon-filled glove box. Lithium metal was used as the anode. The electrolyte was 1 M LiPF_6 with ethylene carbonate/dimethyl carbonate (EC/DMC) (1:1 vol %). Cells were subjected to gal-

vanostatic cycling using a WonAtech system in the voltage range of 4.6 - 3.0 V at rates of 1 - 12 C.

Results and Discussion

Fig. 1 shows X-ray diffraction (XRD) patterns of the pristine and ZrF_x -coated $\text{Li}[\text{Co}_{1/3}\text{Ni}_{1/3}\text{Mn}_{1/3}]\text{O}_2$ powders. The diffraction patterns of the coated powders are identical to those of the pristine sample, despite the presence of a coating layer on the surface. The absence of secondary phases in the entire range of the diffraction patterns corresponding to the coating process may not affect the host structure. It appears that the surface coating layer was formed as an amorphous phase because the heating temperature of 400 °C was not high enough to form a crystalline coating phase. Owing to its open structure, the amorphous coating layer may be beneficial for the transport of Li ions across the surface of the cathode electrode. Fig. 2 shows SEM images of the pristine and ZrF_x -coated $\text{Li}[\text{Co}_{1/3}\text{Ni}_{1/3}\text{Mn}_{1/3}]\text{O}_2$ powders. The crystal faces and edges present on the surface of the pristine $\text{Li}[\text{Co}_{1/3}\text{Ni}_{1/3}\text{Mn}_{1/3}]\text{O}_2$ were very clean and smooth. In contrast, the surface of $\text{Li}[\text{Co}_{1/3}\text{Ni}_{1/3}\text{Mn}_{1/3}]\text{O}_2$ became considerably rough after coating. It could be observed that the coating layer was composed of a large number of nano-particles, which were either distributed independently or connected to each other. Although the nano-particles did not cover the entire surface area of the parent $\text{Li}[\text{Co}_{1/3}\text{Ni}_{1/3}\text{Mn}_{1/3}]\text{O}_2$ powder, the surface area exposed to the electrolyte was greatly reduced due to the coating. SEM-EDS analysis was carried out to investigate the coating layer. Fig. 3 shows EDS spectra dot map of Zr on the ZrF_x -coated $\text{Li}[\text{Co}_{1/3}\text{Ni}_{1/3}\text{Mn}_{1/3}]\text{O}_2$ powders. It was confirmed that Zr was distributed uniformly on the surface of the coated $\text{Li}[\text{Co}_{1/3}\text{Ni}_{1/3}\text{Mn}_{1/3}]\text{O}_2$ powders. An increase in the coating amount leads to an increase in the number of zirconium dots. To investigate the

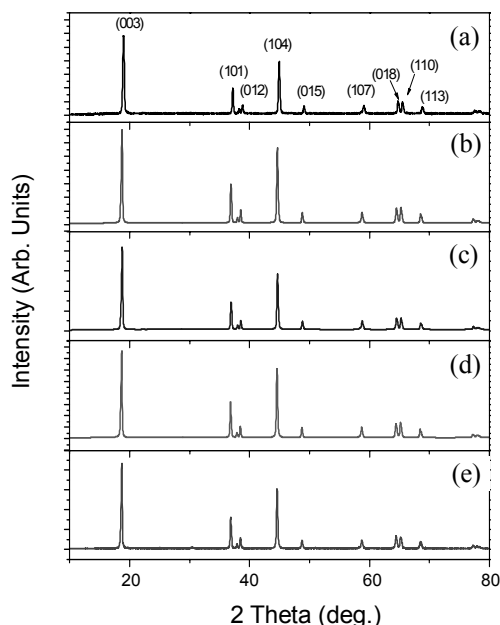


Figure 1. XRD patterns of (a) pristine and (b) 0.25 wt %, (c) 0.5 wt %, (d) 1.0 wt %, and (e) 2.0 wt % ZrF_x -coated $\text{Li}[\text{Ni}_{1/3}\text{Co}_{1/3}\text{Mn}_{1/3}]\text{O}_2$ powders.

shape of the primary particles and the surface morphology in detail transmission electron microscopy (TEM) analysis was carried out. Fig. 4 shows the TEM images of the pristine and 1 wt % ZrF_x -coated $\text{Li}[\text{Co}_{1/3}\text{Ni}_{1/3}\text{Mn}_{1/3}]\text{O}_2$ powders. The surfaces of the pristine sample particles were found to be smooth. Whereas, the surface of the coated $\text{Li}[\text{Co}_{1/3}\text{Ni}_{1/3}\text{Mn}_{1/3}]\text{O}_2$ particle was found to be covered with a thin coating layer with a thickness of approximately 50 - 100 nm. This layer was not continuous throughout. On the basis of the spot pattern observed at the bottom of the TEM image, it is likely that coating layer is the amorphous phase, which is consistent with the result of the XRD analysis. The elements present in the coating layer were confirmed by TEM-EDS analysis, as shown in Fig. 5. The detection of clear peaks corresponding to Zr and F confirmed that the ZrF_x coating layer was successfully formed on the surface of the pristine $\text{Li}[\text{Co}_{1/3}\text{Ni}_{1/3}\text{Mn}_{1/3}]\text{O}_2$ powders. As mentioned earlier, the molar ratio of the Zr source to the F source was adjusted to 1 : 4 for preparation of the coating solution. This was done on the basis of the assumption that the stoichiometric ratio for this compound is ZrF_4 . It was difficult to determine the exact composition of the coating layer, however, the ratio of Zr : F of the coating layer appeared to have changed because of the reaction among the elements of the pristine powder or diffusion into the parent phase.

The electrochemical properties of the coated $\text{Li}[\text{Co}_{1/3}\text{Ni}_{1/3}\text{Mn}_{1/3}]\text{O}_2$ electrodes were compared to those of a pristine electrode. Fig. 6 shows the discharge capacity and cyclic perfor-

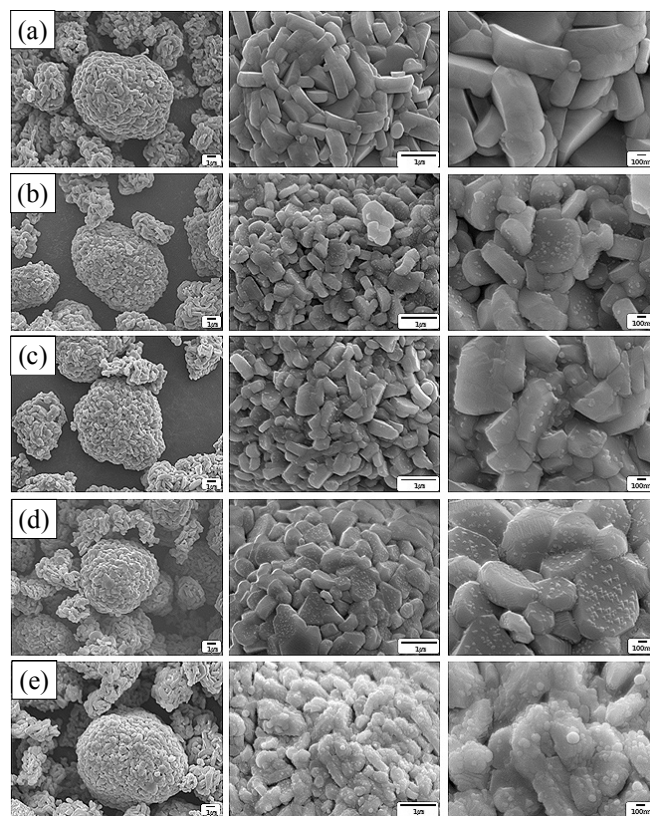


Figure 2. SEM images of (a) pristine and (b) 0.25 wt %, (c) 0.5 wt %, (d) 1.0 wt %, and (e) 2.0 wt % ZrF_x -coated $\text{Li}[\text{Ni}_{1/3}\text{Co}_{1/3}\text{Mn}_{1/3}]\text{O}_2$ powders.

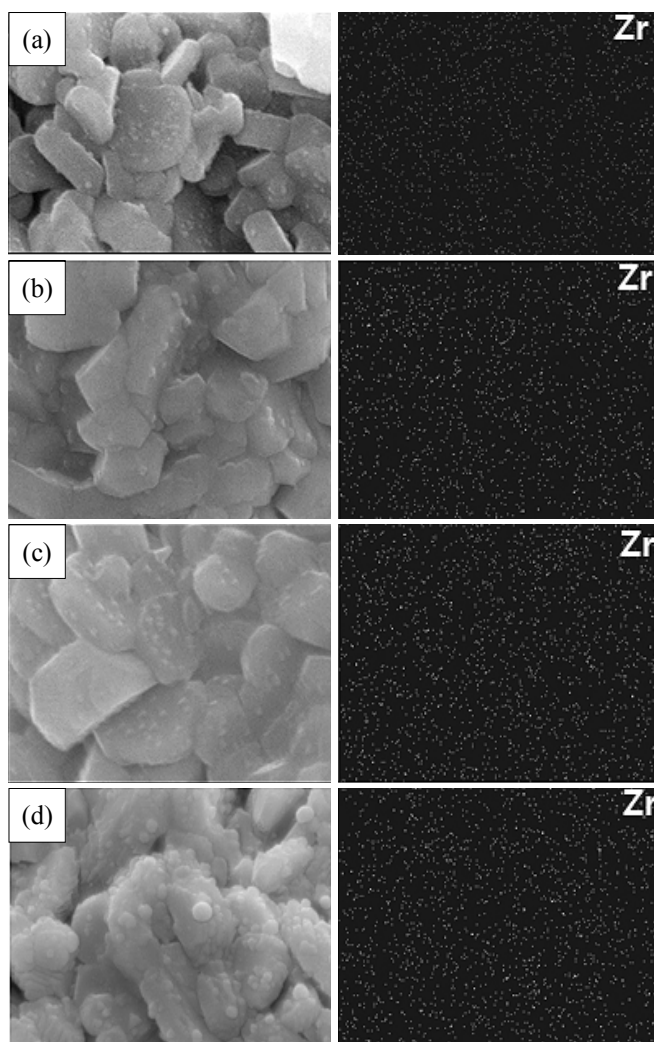


Figure 3. EDS spectra dot maps of Zr in (a) 0.25 wt %, (b) 0.5 wt %, (c) 1.0 wt %, and (d) 2.0 wt % ZrF_x -coated $\text{Li}[\text{Ni}_{1/3}\text{Co}_{1/3}\text{Mn}_{1/3}]\text{O}_2$ powders.

mance of the pristine and coated $\text{Li}[\text{Co}_{1/3}\text{Ni}_{1/3}\text{Mn}_{1/3}]\text{O}_2$ electrodes as a function of charge-discharge rates. The measurement was carried out at 1C, 2C, 4C, 6C, 8C, 10C and 12C rates in the voltage range of 4.6 - 3.0 V. The discharge capacity of the $\text{Li}[\text{Co}_{1/3}\text{Ni}_{1/3}\text{Mn}_{1/3}]\text{O}_2$ electrodes at high C rates was clearly enhanced by 0.25 - 1.0 wt % coating. This implies that ZrF_x coating is an effective approach for improving the rate capability of the $\text{Li}[\text{Co}_{1/3}\text{Ni}_{1/3}\text{Mn}_{1/3}]\text{O}_2$ cathode. The sample with a 0.5 wt % coating showed a much superior rate capability than that with a 0.25 wt % coating. However, as the amount of coating increased to over 1 wt %, the discharge capacity at high C rates was found to decrease. Essentially, the coating layer could be impeding the movement of lithium ions and electrons, because the coating material does not participate in the intercalation-deintercalation process. However, the charge-discharge process is hindered because of the unwanted surface reaction between the electrode and the electrolyte. Moreover, specially, LiPF_6 salt produces HF due to its reaction with humidity in the environment, and therefore, the transition metal (Co, Ni, and Mn) making up the structure of the cathode are dissolved in the electrolyte by the attack

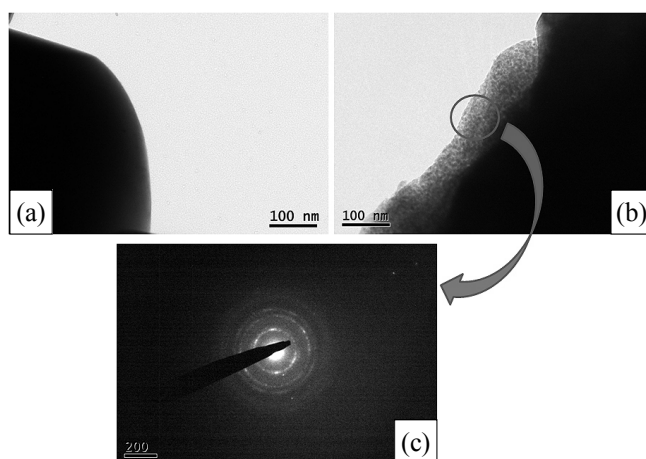


Figure 4. TEM images of (a) pristine cathode, (b) 0.5 wt % of ZrF_x -coated $\text{Li}[\text{Co}_{1/3}\text{Ni}_{1/3}\text{Mn}_{1/3}]\text{O}_2$ cathode, and (c) spot patterns of the area circled in the TEM images.

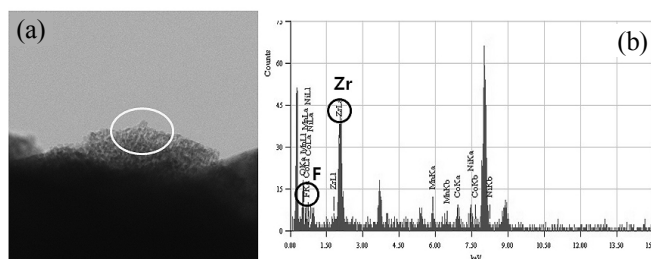


Figure 5. (a) TEM image of coated $\text{Li}[\text{Ni}_{1/3}\text{Co}_{1/3}\text{Mn}_{1/3}]\text{O}_2$ powders, and (b) EDS peaks of coating layer marked in TEM image.

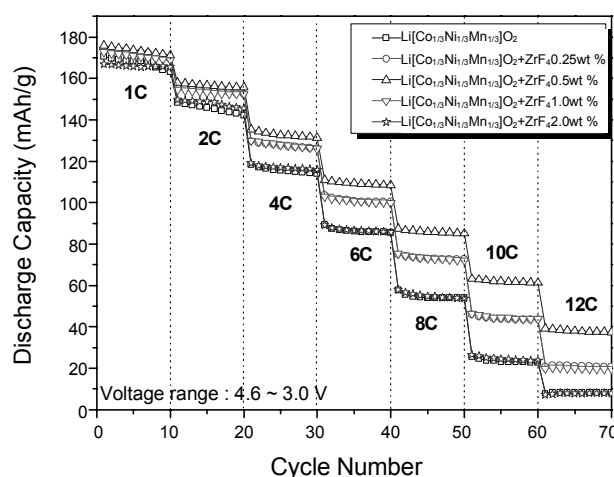


Figure 6. Discharge capacities and cyclic performances of pristine and coated $\text{Li}[\text{Co}_{1/3}\text{Ni}_{1/3}\text{Mn}_{1/3}]\text{O}_2$ electrodes in the voltage range of 4.6 - 3.0 V at 1, 2, 4, 6, 8, and 12 C rates.

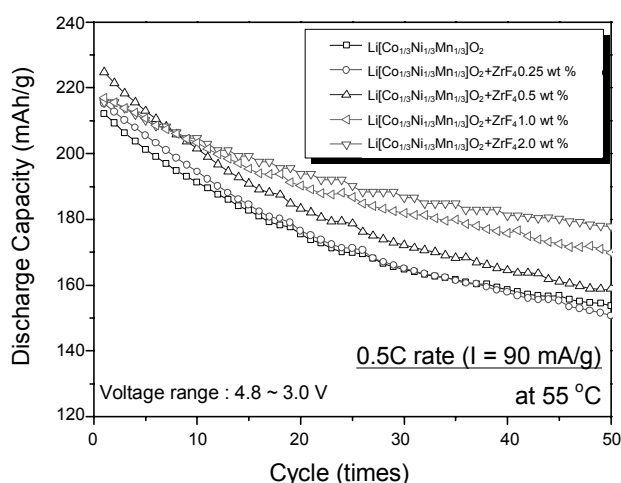
of HF.⁷ Moreover, an unwanted surface interface layer, which interrupts the diffusion of lithium ions and electrons, is formed on the surface of the cathode electrode. A stable coating layer such as ZrF_x can protect the electrode from the reaction with electrolyte by preventing it from direct contact, therefore it may

Table 1. Discharge capacity and capacity retention of $\text{Li}[\text{Ni}_{1/3}\text{Co}_{1/3}\text{Mn}_{1/3}]\text{O}_2$ electrodes at various C rates (values of the first cycle). The percentages indicate the capacity retention compared to the discharge capacity at the 1C rate.

	Pristine (mAh/g)	(%)	ZrF _x 0.25 wt % (mAh/g)	(%)	ZrF _x 0.5 wt % (mAh/g)	(%)	ZrF _x 1.0 wt % (mAh/g)	(%)	ZrF _x 2.0 wt % (mAh/g)	(%)
1C	170.52	100.0	174.00	100.0	175.93	100.0	172.79	100.0	166.87	100.0
2C	148.45	87.1	155.77	89.5	158.02	89.8	154.53	89.4	149.76	89.7
4C	118.32	69.4	129.63	74.5	135.26	76.9	129.95	75.2	119.14	71.4
6C	89.28	52.4	103.56	59.5	110.98	63.1	102.76	59.5	89.24	53.5
8C	57.72	33.8	75.03	43.1	87.33	49.6	75.28	43.6	58.01	34.8
10C	25.43	14.9	45.97	26.4	63.23	35.9	46.39	26.8	26.63	16.0
12C	7.82	4.6	20.79	11.9	39.21	22.3	19.80	11.5	7.13	4.3

Table 2. Discharge capacities and capacity retentions of pristine and ZrF_x-coated $\text{Li}[\text{Ni}_{1/3}\text{Co}_{1/3}\text{Mn}_{1/3}]\text{O}_2$ electrodes during 50 cycles in the voltage range of 4.8 - 3.0 V at 55 °C. The percentages indicate the capacity retention during 50 cycles.

	Pristine (mAh/g)	(%)	ZrF _x 0.25 wt % (mAh/g)	(%)	ZrF _x 0.5 wt % (mAh/g)	(%)	ZrF _x 1.0 wt % (mAh/g)	(%)	ZrF _x 2.0 wt % (mAh/g)	(%)
1	212.16		215.22		224.77		216.94		215.58	
50	153.64	72.4	150.72	70.0	158.86	70.7	169.77	78.3	177.83	82.5

**Figure 7.** Cyclic performances of pristine and ZrF_x-coated $\text{Li}[\text{Co}_{1/3}\text{Ni}_{1/3}\text{Mn}_{1/3}]\text{O}_2$ electrode in the voltage range of 4.8 - 3.0 V at 55 °C.

facilitate lithium diffusion and increase discharge capacity. However, a thicker coating layer may act as an obstacle to the intercalation-deintercalation process. Therefore as the coating concentration increases beyond the optimum concentration, the rate capability deteriorates. Table 1 summarizes the discharge capacity and capacity retention at various C rates (the values of first cycles).

The cyclic performances of pristine and coated $\text{Li}[\text{Co}_{1/3}\text{Ni}_{1/3}\text{Mn}_{1/3}]\text{O}_2$ electrodes were observed, as shown in Fig. 7. In order to clearly illustrate the effect of coating on the cycling behavior under severe measurement condition (high temperature and high cut-off voltage), the upper cut-off voltage and temperature were increased to 4.8 V and 55 °C, respectively. As expected, the discharge capacity of the pristine electrode decreased considerably during cycling in the voltage range of 4.8 - 3.0 V at 55 °C. However, some coated electrode showed enhanced cycle stability compared to the pristine electrode. Table 2 summarizes the dis-

charge capacity and capacity retention under such condition. It is interesting to note that the capacity retention improved with an increase in the amount of coating material. The samples with 0.25 and 0.5 wt % coating showed similar or slightly higher discharge capacities in all cycles, as shown in Fig. 7, however, capacity retention was not enhanced due to coating. In contrast, it is clear that the 1.0 and 2.0 wt % coating electrodes present improved cycling behavior. The capacity retention of the pristine electrode during 50 cycles was just ~72 %. In contrast, the capacity retention values for the 1.0 wt % and 2.0 wt % coating electrodes were ~78 %, and ~83 %, respectively. From this result, it is obvious that the cycling behavior under severe conditions could be improved by surface coating. In particular, a high concentration of coating would be required to achieve cycling stability, because a larger amount of coating material leads to a reduction in the surface of the parent powder, which is directly exposed to the electrolyte. However, the presence of excess coating material (above the optimum concentration) between the particles can lower the electronic and ionic conductivities, resulting in deterioration of the electrochemical properties, as shown in Fig. 6.

Conclusions

ZrF_x was used as a coating material for a $\text{Li}[\text{Co}_{1/3}\text{Ni}_{1/3}\text{Mn}_{1/3}]\text{O}_2$ cathode in order to improve the cathode's electrochemical properties. The formation of a compact coating layer on the surface of pristine particles was observed by SEM and TEM. XRD and TEM analyses confirmed that the coating layer of the samples was an amorphous phase. EDS analysis showed that ZrF_x was distributed uniformly on the surface of the cathode material. Galvanostatic charge-discharge studies at various C rates showed that the ZrF_x coating enhanced the rate capability. This enhancement is due to the presence of a stable ZrF_x coating layer, which effectively suppressed the reactions between the electrode and the electrolyte on the surface of the electrode. However, as

the coating thickness increased over the optimum thickness, the rate capability deteriorated. The cyclic performances of electrodes at high cut-off voltage (4.8 V) and high temperature (55 °C) were also improved by ZrF_x surface coating. In particular, a thick coating layer was more effective in stabilizing the cyclic performance than a thin one.

Acknowledgments. This work was supported by Kyonggi University Research Grant 2008.

References

1. Koyama, Y.; Yabuuchi, N.; Tanaka, I.; Adachi, H.; Ohzuku, T. *J. Electrochem. Soc.* **2004**, *151*, 1545.
2. Yabuuchi, N.; Makimura, Y.; Ohzuku, T. *J. Electrochem. Soc.* **2007**, *154*, A314.
3. Choi, J.; Manthiram, A. *J. Electrochem. Soc.* **2005**, *152*, A1714.
4. Myung, S.-T.; Izumi, K.; Komaba, S.; Sun, Y.-K.; Yashiro, H.; Kumagai, N. *Chem. Mater.* **2005**, *17*, 3695.
5. Noh, M.; Lee, Y.; Cho, J. *J. Electrochem. Soc.* **2006**, *153*, A935.
6. Thackeray, M. M.; Johnson, C. S.; Kim, J. S.; Lauzze, K. C.; Vaughey, J. T.; Dietz, N.; Abraham, D.; Hackney, S. A.; Zeltner, W.; Anderson, M. A. *Electrochem. Commun.* **2003**, *5*, 752.
7. Myung, S.-T.; Izumi, K.; Komaba, S.; Yashiro, H.; Bang, H. J.; Sun, Y. K.; Kumagai, N. *J. Phys. Chem.* **2007**, *C111*, 4061.
8. Lee, H.; Kim, Y.; Hong, Y. S.; Kim, Y.; Kim, M. G.; Shin, N.-S.; Cho, J. *J. Electrochem. Soc.* **2006**, *153*, A781.
9. Ryu, J. H.; Kim, S. B.; Park, Y. J. *Bull. Korean Chem. Soc.* **2009**, *30*, 657.
10. Yun, S. H.; Kim, S. B.; Park, Y. J. *Bull. Korean Chem. Soc.* **2009**, *30*, 1.
11. Park, B.-C.; Kim, H.-B.; Myung, S.-T.; Amine, K.; Belharouak, I.; Lee, S.-M.; Sun, Y. K. *J. Power Sources* **2008**, *178*, 826.
12. Sun, Y. K.; Cho, S.-W.; Lee, S.-W.; Yoon, C. S.; Amine, K. *J. Electrochem. Soc.* **2007**, *154*, A168.
13. Zheng, J. M.; Zhang, Z. R.; Wu, X. B.; Dong, Z. X.; Zhu, Z.; Yang, Y. *J. Electrochem. Soc.* **2008**, *155*, A775.
14. Lim, S.; Cho, J. *J. Electrochem. Commun.* **2008**, *10*, 1478.
15. Hu, S.-K.; Cheng, G.-H.; Cheng, M.-Y.; Hwang, B.-J.; Santhanam, R. *J. Power Sources* **2009**, *188*, 564.